Am. J. Hum. Genet. 49:147–157, 1991

Molecular Characterization of Four Different Classes of Mutations in the Isovaleryl-CoA Dehydrogenase Gene Responsible for Isovaleric Acidemia

Jerry Vockley, Bhama Parimoo, and Kay Tanaka

Department of Human Genetics, Yale University School of Medicine, New Haven, CT

Summary

Isovaleric acidemia (IVA) is an inborn error of leucine metabolism and is caused by a genetically determined deficiency of isovaleryl-CoA dehydrogenase (IVD), a mitochondrial matrix enzyme. IVD is produced as a 45-kDa precursor and then is transported into the mitochondria, where it is processed to its mature 43-kDa size. Previous [^{35}S]methionine-labeling studies of fibroblasts from IVA patients have revealed at least five classes of mutations within the IVD gene. In size, IVD precursor and mature proteins produced by class I mutants are indistinguishable from their normal counterparts. Class II, III, and IV mutants make IVD precursor proteins which are 23 kDa smaller than normal. Subsequent processing in class III and IV mutants is normal but proceeds inefficiently in class II mutants. Class V mutants make no detectable IVD protein. In order to further study these mutations at the molecular level, the IVD coding region from mutant fibroblast cDNA was amplified by the PCR and was analyzed by DNA sequencing. cDNA from class I mutant alleles from two of seven class I mutant cell lines each contained a different missense mutation. In cDNA from a class III mutant, a single base deletion at position 1179 of the coding region was identified which leads to a shift in reading frame, predicting the incorporation of eight abnormal amino acids followed by a premature termination codon. Sequencing of amplified IVD cDNA from a type V mutant has failed to identify any abnormalities. It most probably is deficient in translation of the IVD mRNA. A new class of IVD mutant allele which appears to be transcriptionally defective (type VI) was also identified. Additional study of this set of IVD mutations should add both to our knowledge of the biosynthetic pathway of mitochondrial proteins and to our understanding of the clinical heterogeneity seen in IVA.

Introduction

Isovaleric acidemia (IVA) is an inborn error of leucine metabolism and is caused by a deficiency of isovaleryl-CoA dehydrogenase (IVD; E.C.1.3.99.10) which catalyzes the oxidation of isovaleryl-CoA to 3-methyl-crotonyl-CoA (Tanaka et al. 1966; Rhead and Tanaka 1980). It can present with severe neonatal ketoacidosis leading to death, but in milder cases recurrent episodes of ketoacidosis of varying degree occur later in infancy and childhood.

IVD has been purified to homogeneity from rat and human liver and has been shown to be a tetrameric mitochondrial flavoenzyme with a subunit molecular weight of 43 kDa (Ikeda et al. 1983; Ikeda and Tanaka 1983; Finocchiaro et al. 1988). It is a member of the acyl-CoA dehydrogenase family, a gene family of five enzymes which catalyze the α,β-dehydrogenation of acyl-CoA esters, transferring electrons to electron-transfer flavoprotein (Matsubara et al. 1989). IVD cDNA from rat and human has recently been cloned and sequenced (Matsubara et al. 1989, 1990). In vivo fibroblast studies have shown that IVD mRNA is translated in the cytoplasm as a 45-kDa precursor, is transported into mitochondria, and is processed to its mature form (Ikeda et al. 1987).

Received November 11, 1990; final revision received February 19, 1991.

Address for correspondence and reprints: Jerry Vockley, M.D., Ph.D., Department of Human Genetics, Yale University School of Medicine, 333 Cedar Street, P.O. Box 3333, New Haven, CT 06510.

0002-9297/91/4901-0017$02.00

In a previous study of fibroblast cultures from 15 IVA patients, five classes of variant IVD protein were identified in our laboratory by using [^{35}S]methionine labeling and immunoprecipitation (Ikeda et al. 1985). Type I mutations were most frequent, being found in seven cell lines. In size, type I variant IVD protein was indistinguishable from normal, in both precursor and mature forms, and the former was imported into mitochondria and posttranslationally was processed normally. One cell line produced a precursor IVD protein which was approximately 3 kDa smaller than normal and which was subsequently inefficiently processed. This was designated the *type II variant.* Cells from two Senegalese sibs of nonconsanguineous parents produced a shortened percursor IVD protein which was 2 kDa smaller than normal but which was processed efficiently (type III mutation). The type IV mutant class had a precursor size similar to that of type II but was processed efficiently to mature form. A final class of mutants (i.e., the type V variant) was identified which contained no immunoreactive IVD material. An additional cell line apparently containing both a type I and a type II allele was found. Subsequent studies have shown that mRNA from all of the cell lines was present in normal amounts and was of approximately normal size (Matsubara et al. 1990). In order to characterize the molecular nature of the gene defects responsible for the variant IVD alleles, we have studied IVD cDNA and genomic DNA sequences from normal and mutant fibroblasts by using the PCR (Saiki et al. 1988) and DNA sequencing.

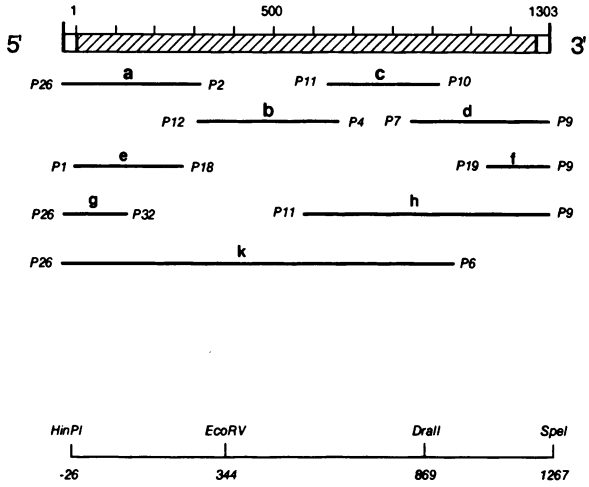

Figure 1 PCR amplification strategy for IVD cDNA and genomic DNA. Initially, the entire IVD cDNA coding region (shown as diagonally hatched area) was amplified, from fibroblast cDNA, in four overlapping fragments (lines a–d), but in later experiments two larger fragments were amplified (lines a + b and c + d). Additional fragments were synthesized to further characterize identified mutants, as described in the text. Oligonucleotides were synthesized according to our previously published IVD cDNA sequence (Matsubara et al. 1990). The sequence and position of the primers used for each amplification are as follows: P1, 1-A→G-30; P2, 288-A→A-317; P4, 603-G→A-637; P6, 947-A→C-918; P7, 948-C→T-977; P9, 1274-T→A-1303; P10, 978-C→C-1007; P11, 573-C→A-602; P12, 258-C→T-287; P18, 287-A→A-268; P19, 1139-G→T-1158; P26, (−34)-T→-(−15); and P32, 144-C→A-125. In some experiments, PCR fragments were subcloned into Bluescript plasmid for further analysis by using *Hin*PI (into the *Acc*I site of the vector), *Eco*RV, *Dra*II, and *Spe*I according to our previously published IVD cDNA sequence (see bottom of figure).

Material and Methods

Fibroblast Cell Culture and mRNA Isolation

Both the sources of IVA fibroblast cell lines and the culture conditions have been described elsewhere (Ikeda et al. 1985; Matsubara et al. 1990). Fibroblast line YH1074 is a normal human diploid cell line containing no known metabolic defect. Mutant cell lines used are as follows: type I, YH501; type III, YH765; type V, YH1339; and YH834, a compound heterozygote for types I and II. One or two roller bottles each of IVA and of control fibroblasts were harvested with trypsin and EDTA, and total RNA was isolated from the pellets by using the guanidinium thiocyanate method (Matsubara et al. 1990). mRNA was purified by oligo-dT chromatography and was stored at −70°C until used.

PCR of cDNA and Genomic DNA

First-strand cDNA was synthesized, with the Riboclone kit (Promega Biotec), from 1–2 μg of fibroblast mRNA by using oligo-dT as primer according to the manufacturer's instructions. One microliter of this reaction mixture was used directly as template for PCR (Saiki et al. 1988). PCR was performed with pairs of specific oligonucleotide primers that were 20 or 30 nucleotides in length, designed to amplify the entire coding region of the 1,269-bp IVD cDNA (fig. 1). Initially the coding region was amplified in four fragments (fig. 1, lines a–d), but in later experiments two larger fragments were amplified (fig. 1, lines a + b and c + d). The reaction mixture contained 10 mM Tris, pH 8.3, 1.5 mM $MgCl_2$, 50 mM KCl, and 0.01 mg gelatin/ml. PCR primers were present at 200 nM each. Cycling was performed in a DNA thermal cycler

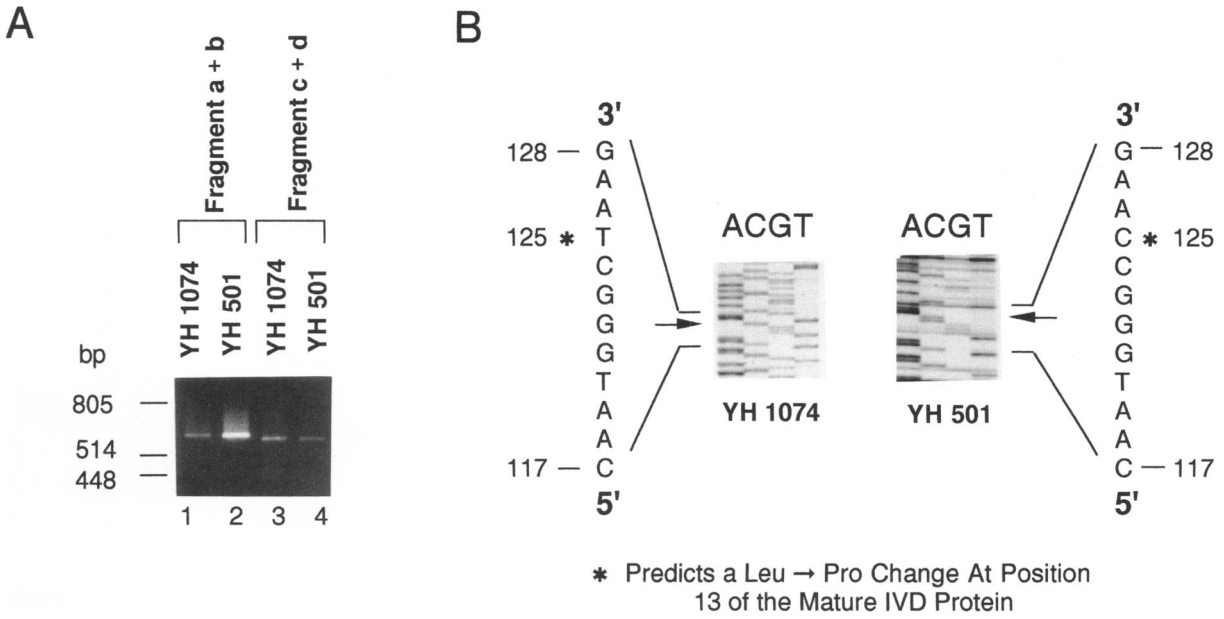

Figure 2 Amplification and sequencing of IVD cDNA from YH501 type I variant fibroblasts. *A*, cDNA from YH1074 (control) and YH501, amplified in two overlapping fragments corresponding to those in fig. 1, lines a + b and c + d. Ten milliliters of the PCR reaction mixture were run on a 1.5% agarose gel containing ethidium bromide and photographed with UV illumination. The expected sizes of the YH1074 and YH501 fragments are 671 and 630 bp, respectively. *B*, Amplified IVD sequences from mutant and control fibroblasts, subcloned as shown in fig. 1 and sequenced. The sequence of one of the subclones corresponding to the *Hin*PI-*Eco*RV fragment from control YH1074 (*left*) and YH501 (*right*) cDNA is shown. The ^{125}T-to-C substitution was present in all six subclones of this fragment analyzed from YH501.

and consisted of 30 cycles, each with a profile of 1 min at 94°C, 2 min at 50°C, and 2 min at 72°C. Ten microliters of the reaction product were analyzed by agarose-gel electrophoresis and were visualized by ethidium bromide staining. PCR fragments were either digested with appropriate restriction endonucleases and subcloned into Bluescript plasmid for further analysis, as shown in figure 1, or were directly sequenced as described below. Additional cDNA fragments were amplified to study specific sequences surrounding an identified mutation, as shown in figure 1 and described in the Results section. Genomic fragments encompassing the mutations identified in YH501 and YH765 IVD cDNA were amplified from normal and mutant fibroblast genomic DNA as above, except that 200 ng of genomic DNA were used as template (fig. 1, lines g and f, respectively).

Sequencing of PCR Fragments

PCR reaction product was separated on a 6% nondenaturing polyacrylamide gel containing 10% glycerol and was stained with 0.5 μg ethidium bromide/ml. The desired fragment was excised from the gel and was recovered by electroelution and then either was subcloned and sequenced or was used as template for PCR to produce single-stranded DNA. PCR conditions to produce single-stranded DNA were as above, except that one of the primers was in 100-fold excess over the other (500 nM/5 nM; Gyllensten and Erlich 1988). Prior to sequencing, PCR product was purified with a Centricon-100 spin dialysis unit (Amicon, Inc.) and then was directly sequenced with the Sequenase enzyme (U.S. Biochemicals, Inc.) by using an appropriate IVD-specific oligonucleotide as primer (Innis et al. 1988). The genomic fragments were reamplified, and the amplified fragments were either subcloned or directly sequenced in the same fashion.

Restriction-Endonuclease Analysis of YH501 cDNA and Genomic DNA

Amplified fragments of YH501 genomic DNA and cDNA surrounding the identified mutation (fig. 1, lines g, and e, respectively) were digested with either restriction endonuclease *Esp*I or restriction endonuclease *Hae*III and were subjected to electrophoresis on a 10% acrylamide gel containing 10% glycerol. The

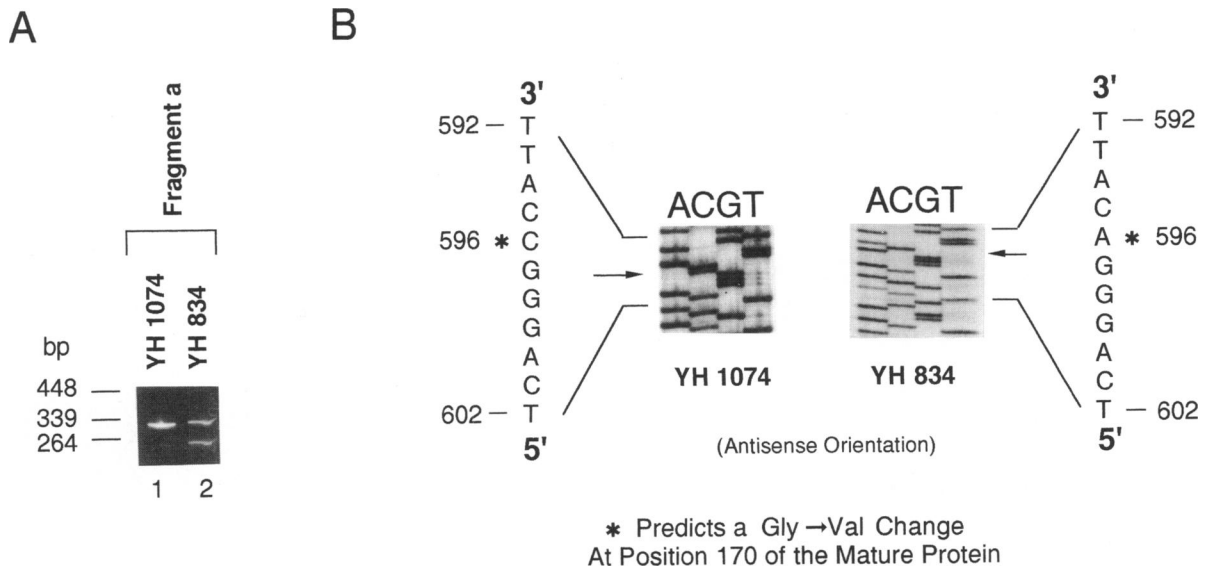

Figure 3 Amplification and sequencing of IVD type I variant cDNA from YH834 fibroblasts. *A*, YH834 IVD cDNA sequences amplified in two overlapping fragments as shown in fig. 1, lines a + b and c + d. IVD sequences corresponding to the 5′ end of the cDNA were reamplified using the primers shown in fig. 1, line a, and were run on a 1.5% agarose gel. The expected fragment size is 313 bp. In lane 2, two bands are detectable; the larger band comigrates with the control (YH1074; lane 1), while the smaller band comigrates with the IVD-specific fragment amplified from YH747 (not shown). *B*, Type I variant IVD sequences either purified by acrylamide gel electrophoresis, reamplified to produce single-stranded DNA, and sequenced directly or subcloned as shown in fig. 1. A sequencing gel in the antisense orientation is shown.

DNA bands were visualized by staining with 0.5 μg ethidium bromide/ml.

Prediction of the Secondary Structure of IVD Protein by Computer Analysis

Predictions of IVD protein secondary structure that were based on cDNA sequence were made with the computer programs PeptideStructure and PlotStructure of the University of Wisconsin Genetics Computer Group (Wolf et al. 1988). Hydrophobicity calculations and secondary-structure predictions were performed according to methods described elsewhere (Garnier et al. 1978; Kyte and Doolittle 1982).

Results

Characterization of Type I Variant IVD

Amplification of IVD-specific cDNA from type I variant YH501 fibroblasts, and electrophoresis on an agarose gel, revealed no differences between the mutant and normal control YH1074 (fig. 2*A*). When cDNA from the type I/type II compound heterozygote cell line YH834 was used as template, two 5′ fragments, one corresponding in size to the control and the other approximately 100 bp smaller than the control, were seen (fig. 3*A*).

PCR-amplified IVD cDNA fragments from YH501 and normal control cDNAs were subcloned into the Bluescript plasmid sites illustrated at the bottom of figure 1 and were sequenced. PCR copies were also directly sequenced. Sequencing of six subclones of each overlapping PCR fragment revealed a consistent single base substitution of a C for a T at position 125 of the IVD-coding sequence from YH501, as compared with the control (fig. 2*B*). Direct sequencing of amplified IVD fragments from YH501 cDNA identified the same single base change.

To isolate the type I variant allele from YH834, cDNA was amplified using the primers shown in figure 1, line k. The type I variant IVD PCR fragment, the larger of the two, was isolated on an acrylamide gel and was reamplified to produce single-stranded DNA. Direct sequencing of this DNA identified a G-to-T transversion at position 596 of the IVD-coding region (fig. 3*B*; a C-to-A transversion in the antisense strand is shown), in contrast to the results in the control. The remaining 3′ portion of the type I IVD from cell line YH834 was analyzed by amplifying it with the primers shown in figure 1, line h, and by sequencing multiple subclones. No consistent sequence changes were seen in these clones.

Both abnormalities were confirmed in at least two

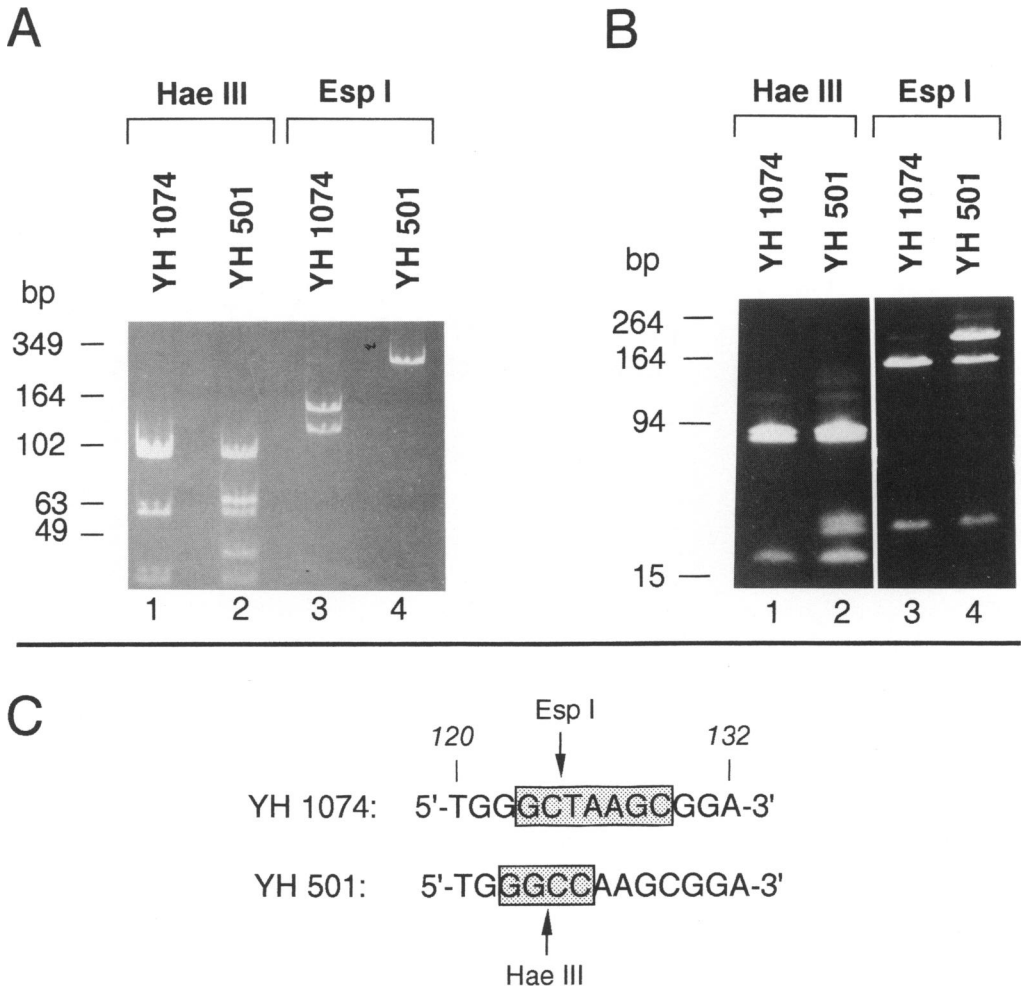

Figure 4 Restriction-endonuclease analysis of YH501 type I variant IVD cDNA and genomic DNA at and surrounding area of ^{125}T-to-C transition. *A*, YH501 IVD cDNA sequences. Sequences were reamplified using primers as in fig. 1, line e, and then were digested with *Hae*III or *Esp*I and run on 10% acrylamide gel. The expected undigested fragment size is 287 bp. Digestion of control IVD cDNA by *Hae*III is predicted to give fragments of 99, 95, 57, 25, and 11 bp, while digestion with *Esp*I yields fragments of 125 and 162 bp. The nucleotide substitution in YH501 is predicted to lead to cleavage of the 99-bp *Hae*III fragment into 62- and 37-bp fragments, while eliminating the sole *Esp*I site. *B*, Exon 1 sequences from control and YH501 genomic DNA sequences were amplified using primers shown in fig. 1, line g, and then were digested with *Hae*III or *Esp*I and run on 12% acrylamide gel. Undigested DNA should give a 178-bp fragment. Control DNA digested with *Hae*III yields 88-, 69-, and 21-bp fragments (lane 1), while *Esp*I should give 151- and 29-bp fragments (lane 3). The ^{125}T-to-C point mutation in YH501 cDNA eliminates the sole *Esp*I site (lane 4) and predicts the cleavage of the 69-bp *Hae*III fragment into 38- and 31-bp fragments (lane 2). C, Restriction-site changes caused by ^{125}T transition. The nucleotide substitution identified in YH501 cDNA predicts both the introduction of a new *Hae*III site after nucleotide 122 and the elimination of the *Esp*I cleavage site at nucleotide position 124.

independent sets of experiments including reverse transcription, PCR, and sequencing using cDNA as template for PCR. The remaining IVD cDNA sequence from both mutant fibroblast lines was identical to the control sequence and differed from our previously published cDNA sequence only by the presence, in both cell lines, of a neutral C-to-T polymorphism at position 1104 of the coding region.

On the basis of the DNA sequencing experiments, YH501 appeared to be expressing a single IVD mutation at the cDNA level, although there was no known parental consanguinity in this case. In order to test whether the patient's IVD cDNA was homogeneous, we took advantage of the alteration of two restriction sites which was produced by the mutation; the introduction of a new *Hae*III site and the loss of an *Esp*I

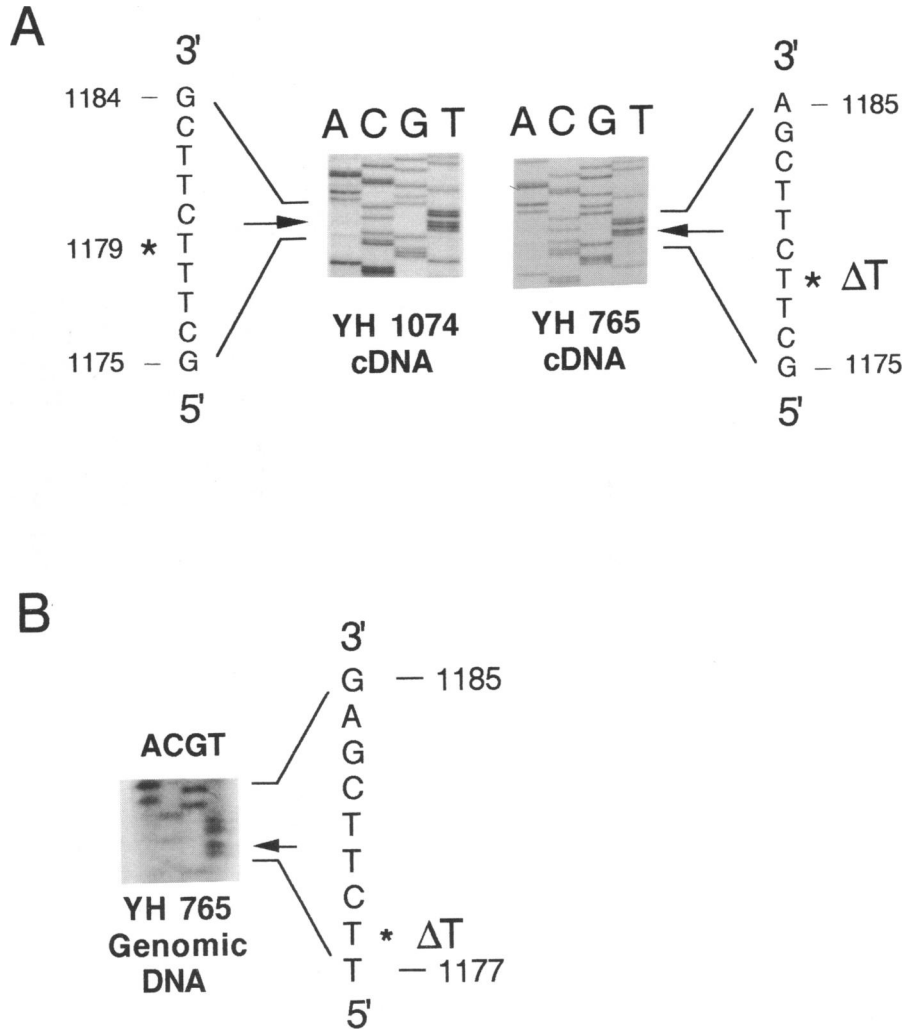

Figure 5 Direct sequencing of IVD type III cDNA and genomic DNA. *A,* Amplified cDNA fragments from YH1074 and YH765. The fragments were excised from agarose gels and were electroeluted, and the recovered fragments were reamplified with additional cycles of PCR to produce double-stranded DNA. The purified PCR products were sequenced directly with the double-stranded technique using Sequenase enzyme. The sequencing ladders shown for YH1074 (*left*) and YH765 fibroblast IVD cDNA (*right*) were obtained by using the IVD-specific primer P19. *B,* Exon 12 fragment containing single T deletion present in YH765. The fragment was amplified from mutant genomic DNA as shown in fig. 1, line f, and was purified by electroelution, reamplified by PCR, and sequenced directly as before, using primer P19.

site (fig. 4*C*) in exon 1 of the IVD gene. A cDNA fragment encompassing positions 1–287 from normal and mutant fibroblasts was amplified with the primers shown in figure 1, line e, and then was digested with these two enzymes. Control IVD cDNA was readily cut by *Esp*I, while YH501 cDNA failed to be cleaved by it (fig. 4*A,* lanes 3 and 4). In contrast, *Hae*III cleaved this fragment of control cDNA in the expected fashion, producing four fragments (the top band is a poorly resolved doublet of 99 and 95 bp), and completely cleaved one band of the top doublet in mutant DNA, producing two new, 62- and 37-bp fragments (fig. 4*A,* lanes 1 and 2). To study this region at the genomic level, exon 1 sequences encompassing the mutation identified in YH501 cDNA were amplified with the primers shown in figure 1, line g. The amplified genomic DNA from the control line contains only a single species corresponding to the expected exon 1 sequence, as shown by complete cleavage with *Esp*I and *Hae*III at the location of the mutation (fig. 4*B;*

lanes 1 and 3). In contrast, DNA amplified from YH501 genomic DNA clearly contains two IVD species present in approximately equal quantities, since the DNA is partially digested, in equimolar amounts, by *Esp*I and *Hae*III (fig. 4*B*, lanes 2 and 4). Thus YH501 appears to be heterozygous for the point mutation at the genomic level, in contrast to the presence of only one IVD species in cDNA. Since the second IVD allele in this cell line is not expressed at the mRNA level, it must either be transcriptionally defective or code for a nuclear RNA that is unstable. We propose to designate this new class of abnormal IVD alleles as the *type VI mutation.*

Characterization of Type III Variant IVD

The size of IVD-specific fragments amplified from type III YH765 cDNA was indistinguishable from that of the control line (not shown). Direct sequencing of the amplified cDNA fragments revealed a deletion of one of a triplet of T residues at positions 1177–1179 of the cDNA sequence, as shown in figure 5*A*. This finding was reproducible in numerous sequencing experiments and was seen in both orientations. This finding was also confirmed on the basis of amplified sequences from three independent reverse-transcription experiments from mutant mRNA. The remainder of both control and mutant IVD cDNA was sequenced in its entirety in both directions and revealed only the silent T-to-C polymorphism at position 1104.

To characterize the T deletion at position 1177–1179 at the genomic level, we amplified a 164-bp fragment from control and mutant fibroblast genomic DNA encompassing part of exon 12 including the position of the deleted base, as shown in figure 1, line f. Direct sequencing of the amplified band from mutant genomic DNA revealed the same single base deletion as was found in mutant cDNA (fig. 5*B*). Normal fibroblast genomic DNA sequence in this region was identical to that of normal cDNA.

Characterization of Type V Variant IVD

In spite of the absence of immunologically cross-reactive IVD protein, the type V IVD cell line, YH1339, contained IVD mRNA that, in both its size and amount, was similar to normal IVD mRNA (Matsubara et al. 1990). Sequencing (in both directions) of 11 subclones of PCR-amplified copies of the IVD cDNA, as well as direct sequence analysis of the amplified fragments from three independent reverse-transcription experiments using this type V IVD mRNA, failed to reveal any consistent abnormality vis-à-vis control IVD mRNA. Negative controls to evaluate the possibility that the PCR reactions had been contaminated with normal cDNA failed to amplify any fragments.

Changes in the IVD Amino Acid sequence That Are Caused by Mutations, and Computer-aided Predictions of Normal and Mutant IVD Protein Structures

The ^{125}T-to-C transition identified in YH501 mutant cDNA codes for the change of a Leu residue to a Pro at position 13 of the mature IVD protein (residue 42 of the precursor). Computer analysis of this altered amino acid sequence predicts the introduction of a new turn of greater than 180° in the protein backbone, compared with normal IVD (fig. 6). The ^{596}G-to-T transversion seen in the type I variant IVD allele from YH834 predicts the alteration of amino acid residue 170 of the mature IVD protein (position 198 of the precursor) from Gly to Val. Computer analysis of the possible effects that this mutation might have on IVD protein secondary structure were unrevealing.

The single base deletion at position 1179 in YH765 type III IVD introduces a shift in reading frame, leading to the incorporation of eight abnormal amino acids after ^{393}Phe of the precursor IVD (position 364 of the mature protein), followed by premature termination of translation (fig. 7). The mutant protein is thus 22 amino acids shorter than its normal counterpart. Computer predictions of the effect that these changes might have on IVD protein secondary structure are shown in figure 8. Compared with the normal protein, the carboxy terminal of the mutant protein is predicted to be drastically altered, with both shortening of the tail and the introduction of a new turn in the protein backbone.

Discussion

At least five known classes of variant IVD genes have previously been identified at the polypeptide level (Ikeda et al. 1985). We have previously reported that in type II IVA fibroblasts a splicing error in IVD RNA leads to the deletion of exon 2 sequences from IVD mRNA and of 30 amino acids from IVD protein and results in inefficient mitochondrial processing of the precursor IVD (Vockley et al. 1990). The current study explores the molecular basis for three additional mutant classes and identifies a new type of mutant allele which we designate as type VI. These data are summarized in table 1. In our previous study of variant IVD protein, the type I allele was most frequent. The

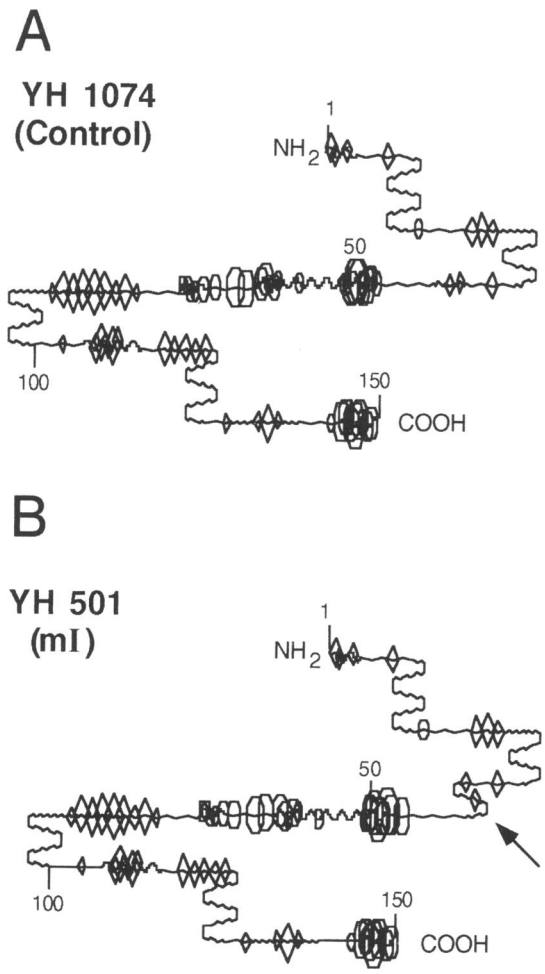

Figure 6 Computer-assisted prediction of secondary structure of type I IVD mutant protein. Kyte-Doolittle and Garnier-Robson predictions of normal mutant IVD protein secondary structures were performed with the PeptideStructure and PlotStructure programs of the University of Wisconsin Genetics Computer Group (Wolf et al. 1988). The predicted structures shown represent the 150 amino terminal amino acids of the normal (*A*) and mutant YH501 (*B*) precursor proteins. Diamonds represent areas of Kyte-Doolittle hydrophobicity which, when averaged over nine amino acids, are greater than 1.3, and octagons correspond to regions of Kyte-Doolittle hydrophilicity which, when averaged over nine amino acids, are greater than 1.3. Helices are indicated by a sine wave, and β sheets are indicated by a sawtooth wave. The amino acid numbering starts with the first residue of the leader peptide as 1. The arrow points to the structurally abnormal region of YH501 IVD protein.

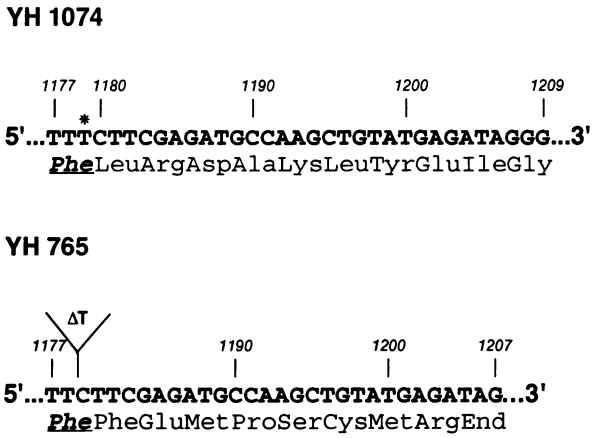

Figure 7 Predicted carboxy-terminal amino acid sequence of normal and type III mutant IVD protein. The single T deletion, at positions 1177–1179, identified in YH765 IVD cDNA leads to a predicted frameshift, causing the incorporation of eight abnormal amino acids following ^{393}Phe of the IVD precursor (^{364}Phe of the mature IVD protein), and then to premature termination of translation (see bottom of figure). The normal sequence is shown in the top portion of the figure.

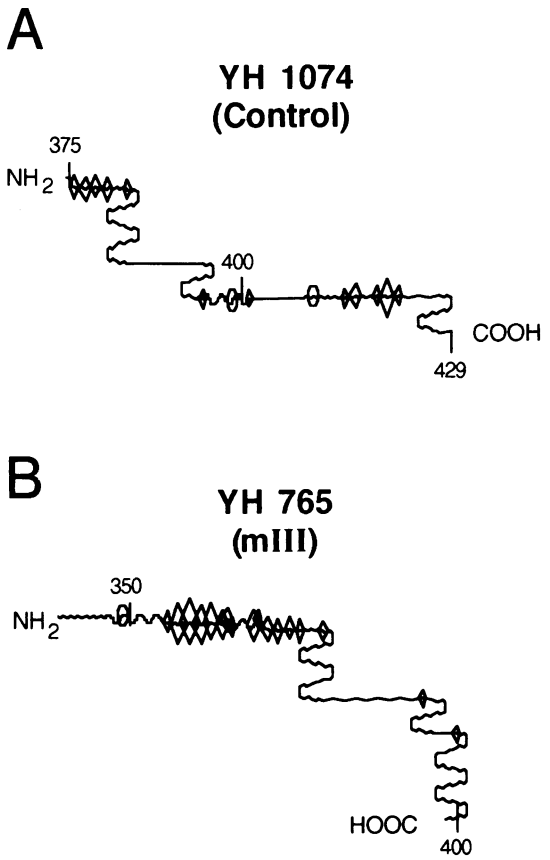

Figure 8 Computer-assisted prediction of secondary structure of type III IVD mutant protein. Kyte-Doolittle and Garnier-Robson predictions of the normal and mutant IVD protein secondary structures were performed as described in the legend to fig. 6. The secondary structure of the carboxy-terminal 55 amino acids of normal (*A*) and mutant (*B*) YH765 precursor proteins are shown. The amino acid numbering starts with the first residue of the leader peptide as 1.

Table 1

Molecular Characterization of Various IVA Alleles

Variant	Variant Protein			Molecular Changes	
	Size	Posttranslational Processing	Sequence Alteration[a]	At mRNA Level	At Gene Level
Type I: YH501 and YH834....	Normal	Normal	Heterogenous substitution—YH501, ^{13}Leu→Pro; and YH834, ^{170}Gly→Val	Heterogenous point mutations—YH501, ^{125}T→C; and YH834, ^{596}G→T	Corresponding change in gene
Type II: YH747 and YH834...	Truncated: 3 kDa shorter	Inefficiently processed	30-Amino-acid deletion (^{20}Leu→^{49}Arg)	Splicing error leading to 90-nucleotide deletion, from ^{145}C to ^{234}A (entire second coding exon)	Primary change in gene is unknown
Type III: YH765	Truncated: 2 kDa shorter	Normal	Eight abnormal amino acids after ^{364}Phe, terminates at position 372	^{1179}T Deletion, causing frame shift, followed by eight abnormal codons and premature stop codon	Corresponding change in gene
Type V: YH1339	CRM negative	NA	NA	Normal coding region Probable translation defect	Cause unknown
Type VI: YH747 and YH834..	CRM negative	NA	NA	No mRNA	Probable transcription defect

Note.—NA = not applicable.

[a] Superscript number indicates position in mature IVD protein.

CRM-negative type V allele was the second most frequent, with two cell lines apparently homozygous for this allele. However, the frequency of type V may be higher than that predicted by the results of the variant IVD protein analysis, since some cell lines that, by protein-labeling studies, appear to be homozygous for the type I, type II, type III, or type IV alleles may actually be compound mutants for the allele and a type V.

Type I variant IVD precursor protein was previously shown to be of normal size and to be transported into mitochondria and processed to a mature form in a manner indistinguishable from that seen in control fibroblasts. Thus this class of variant alleles was postulated to represent point mutations (Ikeda et al. 1985). Our findings substantiate this hypothesis for each of the two type I variant IVD alleles characterized in YH501 and YH834. Furthermore, the point mutations in these two cell lines were different, suggesting the heterogeneous nature of this group. It should be noted that the substitution seen in the type I allele in YH834 is consistent with a mutational mechanism of mismatch pairing, between a methyl-cytosine residue of a CpG dinucleotide with a T, during DNA replication (Barker et al. 1984).

We were initially surprised to find that YH501 appeared to be expressing only a single abnormal IVD allele at the cDNA level, thereby mimicking homozygosity. However, at the genomic level, a second IVD allele was identified. Since the coding sequence of this second variant IVD allele is entirely normal but not expressed at the mRNA level, the second abnormal allele must either be transcriptionally defective or code for a nuclear RNA that cannot be processed and is therefore degraded. Therefore, it represents a new class of aberrant IVD genes. We propose to designate this as type VI. It is possible, but not necessary, that the type VI allele in YH501 is identical to the second abnormal allele identified in the YH747 cell line (Vockley et al. 1989). Similarly, some of the CRM-negative cell lines previously classified as type V mutants may, in fact, also contain a type VI allele. Sequence information about both the 5′-untranslated region and all intron/exon junctions of the mutant IVD gene is necessary to identify the change responsible for the type VI defect.

At present, little is known about structure/function relationships within the IVD protein. Thus, the precise nature of the effect of the identified IVD mutations is unknown. In considering the importance of these mutations, we find that it is useful to note that various acyl-CoA dehydrogenases share numerous identical and conserved amino acid residues throughout their sequences, except in the leader peptide and in the N-terminal region (Matsubara et al. 1989). The universal distribution of the identical and conserved residues suggests that their tertiary structures are rigidly and similarly constructed. While X-ray crystallographic study of IVD protein has not been performed, porcine MCAD has been studied at 3Å resolution (Kim and Wu 1988). The ^{13}Leu and ^{170}Gly residues that are altered in the mature type I IVD protein in YH501 and YH834, respectively, are both conserved in three of four acyl-CoA dehydrogenases of the gene family in both rats and humans, underscoring their importance. By comparison with the tertiary structure or porcine MCAD, the abnormal amino acid residue in the type I IVD in YH834 lies in a region of β-pleated sheet that forms part of the crevice that contains FAD binding and accommodates substrate, and thus it may affect interaction between the apoenzyme and these two molecules. The mutation in YH501 IVD drastically alters the mutant protein's predicted protein backbone secondary structure near the amino terminus, a region we have recently suggested may be important in substrate binding for members of this gene family (Matsubara et al. 1989).

The molecular basis of the type III abnormality is a single base deletion near the 3′ end of the IVD gene, causing a frame shift and producing eight abnormal amino acid codons and a premature stop signal. The predicted 22-amino-acid difference between the size of the type III IVD protein and that of its normal counterpart is in good agreement with the apparent 2-kDa size difference seen on SDS-PAGE gels. This mutation has been confirmed to be present in homozygous fashion in the genomic DNA of mutant fibroblasts. The effective posttranslational processing of variant IVD protein in type III IVA cells is in distinct contrast to the findings in type II IVA fibroblasts. Since the carboxy-terminal domain of IVD is considered, in analogy to porcine MCAD, to participate in tetramerization of the mature subunit, it is possible that the drastic change seen in this region of type III IVD protein causes the impairment of tetramer formation, leading to instability of the protein.

Finally, type V cell line YH1339 had previously been shown to produce no immunologically detectable IVD protein (Ikeda et al. 1985). Both direct sequencing of all amplified IVD PCR fragments and sequenc-

ing of numerous subclones of these fragments failed to reveal any abnormality at the cDNA level. Thus, the nature of this mutation remains unclear.

Acknowledgments

mRNA from IVA cells was prepared by Drs. Yoichi Matsubara and Yasuyuki Ikeda and by Susan Keese. Oligonucleotides were synthesized by Dr. John Florey, Department of Human Genetics, Yale University School of Medicine. This work was supported by NIH grant DK 17453 and by March of Dimes grant 1-1230. J.V. was supported in part by Public Health Service grants GM 13125 and GM 07439. We wish to thank Connie Woznick for her assistance in preparation of the manuscript.

References

Barker D, Schafer M, White R (1984) Restriction sites containing CpG show a higher frequency of polymorphism in human DNA. Cell 36:131–138

Finocchiaro G, Ito M, Tanaka K (1988) Purification and properties of short chain, medium chain and isovaleryl acyl-CoA dehydrogenases from human liver. J Biol Chem 263:15773–15780

Garnier J, Osguthorpe DJ, Robson B (1978) Analysis of the accuracy and implications of simple methods for predicting the secondary structure of globular proteins. J Mol Biol 120:97–120

Gyllensten UB, Erlich HA (1988) Generation of single-stranded DNA by the polymerase chain reaction and its application to direct sequencing of the HLA-DQA locus. Proc Natl Acad Sci USA 85:7652–7656

Ikeda Y, Dabrowski C, Tanaka K (1983) Separation and properties of five distinct acyl-CoA dehydrogenases from rat liver mitochondria. J Biol Chem 258:1066–1076

Ikeda Y, Keese S, Fenton WA, Tanaka K (1987) Biosynthesis of four rat liver mitochondrial acyl-CoA dehydrogenases: import into mitochondria and processing of their precursors in a cell-free system and in cultured cells. Biochem Biophys 252:662–674

Ikeda Y, Keese S, Tanaka S (1985) Molecular heterogeneity of variant isovaleryl acyl-CoA dehydrogenase from cultured isovaleric acidemia fibroblasts. Proc Natl Acad Sci USA 82:7081–7085

Ikeda Y, Tanaka K (1983) Purification and characterization of isovaleryl co-enzyme A dehydrogenase from rat liver mitochondria. J Biol Chem 258:1077–1085

Innis MA, Myambo KB, Gelfand DH, Brow MAD (1988) DNA sequencing with *Thermus aquaticus* DNA polymerase and direct sequencing of polymerase chain reaction amplified DNA. Proc Natl Acad Sci USA 85:9436–9440

Kim J-J, Wu J (1988) Structure of the medium chain acyl-CoA dehydrogenase from pig liver mitochondria at 3-Å resolution. Proc Natl Acad Sci USA 84:6677–6681

Kyte J, Doolittle RF (1982) A simple method for displaying the hydropathic character of a protein. J Mol Biol 157: 105–132

Matsubara Y, Indo Y, Naito E, Ozasa H, Glassberg R, Vockley J, Ikeda Y, et al (1989) Molecular cloning and nucleotide sequence of cDNAs encoding the precursors of rat long chain acyl-CoA, short chain acyl-CoA, and isovaleryl CoA dehydrogenases: sequence homology of four enzymes of the acyl-CoA dehydrogenase family. J Biol Chem 264:16321–16331

Matsubara Y, Ito M, Glassberg R, Satyabhama S, Ikeda Y, Tanaka K (1990) Nucleotide sequence of mRNA encoding human isovaleryl-coenzyme A dehydrogenase and its expression in isovaleric acidemia fibroblasts. J Clin Invest 85:1058–1064

Rhead WJ, Tanaka K (1980) Demonstration of a specific mitochondrial isovaleryl-CoA dehydrogenase deficiency in fibroblasts from patients with isovaleric acidemia. Proc Natl Acad Sci USA 77:580–583

Saiki R, Gelfand D, Stoffel S, Scharf S, Higuchi R, Horn R, Mullis K, et al (1988) Primer-directed enzymatic amplification with a thermostable DNA polymerase. Science 239:487–491

Tanaka K, Budd MA, Efron ML, Isselbacher KJ (1966) Isovaleric acidemia: a new genetic defect of leucine metabolism. Proc Natl Acad Sci USA 56:236–242

Vockley J, Matsubara Y, Ikeda Y, Tanaka K (1989) Identification of molecular defects responsible for isovaleric acidemia. Am J Hum Genet 45 [Suppl]: A227

Wolf H, Modrow M, Motz B, Hameson B, Hermann B, Forsch B (1988) An integrated family of amino acid sequence analysis programs. Comput Appl Biosci 4:187–191